

A peer-reviewed version of this preprint was published in PeerJ on 17 May 2017.

[View the peer-reviewed version](https://peerj.com/articles/3290) (peerj.com/articles/3290), which is the preferred citable publication unless you specifically need to cite this preprint.

Allen KA, Bruno JF, Chong F, Clancy D, McClanahan TR, Spencer M, Żychaluk K. 2017. Among-site variability in the stochastic dynamics of East African coral reefs. PeerJ 5:e3290
<https://doi.org/10.7717/peerj.3290>

Among-site variability in the stochastic dynamics of East African coral reefs

Katherine A Allen^{1,2}, John F Bruno³, Fiona Chong¹, Damian Clancy⁴, Tim R McClanahan⁵, Matthew Spencer^{Corresp., 1}, Kamila Zychaluk⁶

¹ School of Environmental Sciences, University of Liverpool, Liverpool, United Kingdom

² Institute of Integrative Biology, University of Liverpool, Liverpool, United Kingdom

³ Department of Biology, University of North Carolina at Chapel Hill, Chapel Hill, North Carolina, United States

⁴ School of Mathematical and Computer Sciences, Actuarial Mathematics and Statistics, Heriot-Watt University, Edinburgh, United Kingdom

⁵ Wildlife Conservation Society, New York, United States

⁶ Department of Mathematical Sciences, University of Liverpool, Liverpool, United Kingdom

Corresponding Author: Matthew Spencer
Email address: m.spencer@liverpool.ac.uk

Coral reefs are dynamic systems whose composition is highly influenced by unpredictable biotic and abiotic factors. Understanding the spatial scale at which long-term predictions of reef composition can be made will be crucial for guiding conservation efforts. Using a 22-year time series of benthic composition data from 20 reefs on the Kenyan and Tanzanian coast, we developed Bayesian vector autoregressive state-space models for reef dynamics, incorporating among-site variability, and quantified their long-term behaviour. We estimated that if there were no among-site variability, the total long-term variability would be approximately one third of its current value. Thus, our results showed that among-site variability contributes more to long-term variability in reef composition than does temporal variability. Individual sites were more predictable than previously thought, and predictions based on current snapshots are informative about long-term properties. Our approach allowed us to identify a subset of possible climate refugia sites with high conservation value, where the long-term probability of coral cover ≤ 0.1 was very low. Analytical results show that this probability is most strongly influenced by among-site variability and by interactions among benthic components within sites. These findings suggest that conservation initiatives might be successful at the site scale as well as the regional scale.

1 Among-site variability in the stochastic dynamics of East African coral
2 reefs

3 Katherine A. Allen

4 *School of Environmental Sciences, University of Liverpool, Liverpool, L69 3GP, UK **

5 John F. Bruno

6 *Department of Biology, University of North Carolina at Chapel Hill, Chapel Hill, North Carolina 27599-3300, USA †*

7 Fiona Chong

8 *School of Environmental Sciences, University of Liverpool, Liverpool, L69 3GP, UK ‡*

9 Damian Clancy

10 *School of Mathematical and Computer Sciences, Actuarial Mathematics and Statistics, Heriot-Watt University, Edinburgh, UK §*

11 Tim R. McClanahan

12 *Wildlife Conservation Society, 2300 Southern Boulevard, Bronx, NY 10460, USA ¶*

13 Matthew Spencer

14 *School of Environmental Sciences, University of Liverpool, Liverpool, L69 3GP, UK ||*

15 Kamila Żychaluk

16 *Department of Mathematical Sciences, University of Liverpool, Liverpool, L69 7ZL, UK ***

*k.a.allen@liverpool.ac.uk. Current address: Institute of Integrative Biology, University of Liverpool, Liverpool L69 7ZB, UK

†jbruno@unc.edu

‡f.chong@student.liverpool.ac.uk

§d.clancy@hw.ac.uk

¶tmccclanahan@wcs.org

||Corresponding author: m.spencer@liverpool.ac.uk

**kamila.zychaluk@liverpool.ac.uk

17 **Abstract**

18 Coral reefs are dynamic systems whose composition is highly influenced by unpredictable biotic
19 and abiotic factors. Understanding the spatial scale at which long-term predictions of reef
20 composition can be made will be crucial for guiding conservation efforts. Using a 22-year time
21 series of benthic composition data from 20 reefs on the Kenyan and Tanzanian coast, we
22 developed Bayesian vector autoregressive state-space models for reef dynamics, incorporating
23 among-site variability, and quantified their long-term behaviour. We estimated that if there were
24 no among-site variability, the total long-term variability would be approximately one third of its
25 current value. Thus, our results showed that among-site variability contributes more to long-term
26 variability in reef composition than does temporal variability. Individual sites were more
27 predictable than previously thought, and predictions based on current snapshots are informative
28 about long-term properties. Our approach allowed us to identify a subset of possible climate
29 refugia sites with high conservation value, where the long-term probability of coral cover ≤ 0.1
30 was very low. Analytical results show that this probability is most strongly influenced by
31 among-site variability and by interactions among benthic components within sites. These findings
32 suggest that conservation initiatives might be successful at the site scale as well as the regional
33 scale.

34 Introduction

35 “Probabilistic language based on stochastic models of population growth” has been proposed as a
36 standard way to evaluate conservation and management strategies (Ginzburg et al., 1982). For
37 example, a stochastic population model can be used to estimate the probability of abundance
38 falling below some critical level. Such population viability analyses are widely used, and may be
39 reasonably accurate if sufficient data are available (Brook et al., 2000). In principle, the same
40 approach could be used for communities, provided that a sufficiently simple model of community
41 dynamics can be found.

42 A good candidate for such a model is the vector autoregressive model of order 1 or VAR(1)
43 (Lütkepohl, 1993; Ives et al., 2003). This is a discrete-time model for the vector of log
44 abundances of a set of species or groups, which includes environmental stochasticity and may
45 include environmental explanatory variables. It makes the simplifying assumptions that inter- and
46 intraspecific interactions can be represented by a linear approximation on the log scale, and that
47 future abundances are conditionally independent of past abundances, given current abundances.
48 Where possible, it is desirable to use a state-space form of the VAR(1) model, which also includes
49 measurement error (Lindgren et al., 2009; Mutshinda et al., 2009).

50 Hampton et al. (2013) review applications of VAR(1) models in community ecology, which
51 include studying the stability of freshwater plankton systems (Ives et al., 2003), designing
52 adaptive management strategies for the Baltic Sea cod fishery (Lindgren et al., 2009), and
53 estimating the contributions of environmental stochasticity and species interactions to temporal
54 fluctuations in abundance of moths, fish, crustaceans, birds and rodents (Mutshinda et al., 2009).
55 Recently, VAR(1) models have been applied to the dynamics of the benthic composition of coral
56 reefs (Cooper et al., 2015; Gross and Edmunds, 2015), using a log-ratio transformation (Egozcue
57 et al., 2003) rather than a log transformation, to deal with the constraint that proportional cover of
58 space-filling benthic groups sums to 1.

59 Coral reefs are dynamic systems influenced by both deterministic factors such as interactions
60 between macroalgae and hard corals (Mumby et al., 2007), and stochastic factors such as

61 temperature fluctuations (Baker et al., 2008) and storms (Connell et al., 1997), and are classic
62 examples of non-equilibrium systems whose diversity is determined by both interspecific
63 interactions and disturbance (Huston, 1985). In general, high coral cover is considered a desirable
64 state for a coral reef, and there is some evidence that coral cover of at least 0.1 is important for
65 long-term maintenance of reef function (Kennedy et al., 2013; Perry et al., 2013; Roff et al.,
66 2015), although this threshold may differ among reefs dominated by different coral genera (Perry
67 et al., 2015). Thus, coral cover of 0.1 might be an appropriate threshold against which to evaluate
68 reef conservation strategies, and VAR(1) models can be used to estimate the probability of coral
69 cover falling to or below this threshold (Cooper et al., 2015).

70 There is evidence for systematic differences in reef dynamics among locations. For example, on
71 the Great Barrier Reef up to 2012, coral cover had declined more strongly at southern and central
72 than at northern sites (De'ath et al., 2012), and in the U.S. Virgin Islands, VAR(1) models showed
73 that sites differed in their sensitivity to disturbance and speed of recovery (Gross and Edmunds,
74 2015). Some sites in a region may therefore represent coral refugia, where reefs are either
75 protected from or able to adapt to changes in environmental conditions (McClanahan et al., 2007).
76 Alternatively, apparent differences among sites may simply be due to differences in recent
77 disturbance history. Although it may be possible to associate differences in dynamics among sites
78 with differences in environmental variables, it is also possible to treat among-site differences as
79 another random component of a VAR(1) model. This will allow estimation of the relative
80 importance of among-site variability and within-site temporal variability, which is important for
81 the design of conservation strategies. If within-site temporal variability dominates, it will not be
82 possible to identify good sites to conserve based on current status, while if among-site variability
83 dominates, even a "snapshot" sample at one time point may be enough to identify good sites.
84 Thus, for example, the reliability of among-site patterns from surveys at one time point, such as
85 the relationship between benthic composition and human impacts on remote Pacific atolls (Sandin
86 et al., 2008), depends on among-site variability dominating within-site temporal variability. Thus,
87 even though a simple strategy based on a snapshot may turn out to be effective, it is not possible

88 to know this in advance of carrying out a more sophisticated analysis that treats the system as
89 dynamic. Furthermore, since among-site variability will affect the probability of undesirable
90 community composition (such as coral cover ≤ 0.1), conservation strategies that explicitly
91 address among-site variability may be effective. As far as we know, the use of VAR(1) models to
92 estimate spatiotemporal heterogeneity and identify refugia is novel, although other applications of
93 VAR(1) models with random subject effects exist (e.g. Gorrostieta et al., 2012; Driver et al.,
94 2016). Our approach differs from existing methods for identifying refugia (Keppel et al., 2012) in
95 that it explicitly focuses on spatial variability in dynamics over ecological timescales, rather than
96 on patterns that are static or vary only over much longer timescales. Furthermore, rather than
97 differences in physical factors (West and Salm, 2003), we focus on differences in community
98 dynamics.

99 Here, we develop a state-space VAR(1) model for regional dynamics of East African coral reefs,
100 including random site effects and measurement error, and use it to answer four key questions
101 about spatial and temporal variability. How important is among-site variability in the dynamics of
102 benthic composition, relative to within-site temporal variability? How much variability is there
103 among sites in the probability of low (≤ 0.1) coral cover? Which model parameters have the
104 largest effects on the probability of low coral cover in the region? How informative is a single
105 snapshot in time about the long-term properties of a site?

106 **Methods**

107 **Data collection**

108 Surveys of 20 spatially distinct reefs in Kenya and Tanzania (supporting information, Table A1,
109 Figure A1) were conducted annually during the period 1991-2013 (generally in November or
110 December prior to 1998, but January or February from 1998 onwards). Those in the north were
111 typically fringing reefs, 100 m to 2000 m from the shore, while those in the south were typically
112 smaller and more isolated patch reefs, further from the shore (McClanahan and Arthur, 2001). We

113 categorized reefs as either fished or unfished, although there was substantial heterogeneity within
114 these categories, because some fished reefs were community management areas with reduced
115 harvesting intensity (Cinner and McClanahan, 2015), and some unfished reefs had only recently
116 been designated as reserves. Of the 20 reefs, 10 were divided into two sites separated by 20 m to
117 100 m, while the remaining 10 reefs comprised only one site. The selection of sites represents
118 available data rather than a random sample from all the locations at which coral reefs are present
119 in the geographical area (and all of the longest time series are from Kenyan fringing reefs). Thus,
120 when we refer below to ‘a randomly-chosen site’ we strictly mean ‘a site drawn at random from
121 the population for which data could have been available.’

122 Each of the 30 sites was visited at least twice (data from sites visited once were omitted), with a
123 maximum of 20 visits. A version of line-intercept sampling (Kaiser, 1983; McClanahan et al.,
124 2001) was used to estimate reef composition. In total, 2665 linear transects were sampled across
125 all sites and years, with between 5 and 18 transects (median 9) at each site in a single year.
126 Transects were randomly placed between two points 10m apart, but as the transect line was
127 draped over the contours of the substrate, the measured lengths varied between 10m and 15 m.
128 Cover of benthic taxa was recorded as the sum of draped lengths of intersections of patches of
129 each taxon with the line, divided by the total draped length of the line. Intersections with length
130 less than 3 cm were not recorded. Taxa were identified to species or genus level, but for this study
131 cover was grouped into three broad categories: hard coral, macroalgae and other (algal turf,
132 calcareous and coralline algae, soft corals and sponges). Sand and seagrass were recorded, but
133 excluded from our analysis, which focussed on hard substrate. The dynamics of a subset of these
134 data were analyzed using different methods in Żychaluk et al. (2012).

135 **Data processing**

136 The three cover values form a three-part composition, a set of three positive numbers whose sum
137 is 1 (Aitchison, 1986, Definition 2.1, p. 26). Standard multivariate statistical techniques are not
138 appropriate for untransformed compositional data, due to the absence of an interpretable

139 covariance structure and the difficulties with parametric modelling (Aitchison, 1986, chapter 3).
 140 To avoid these difficulties, the proportional cover data were transformed to orthogonal,
 141 unconstrained, isometric log-ratio (ilr) coordinates (Egozcue et al., 2003). It is of course true that
 142 the model presented below for transformed data has an analogous model for untransformed data
 143 (Mateu-Figueras et al., 2011). However, working with transformed data allows us to use familiar
 144 methods.
 145 The transformed data at site i , transect j , time t were represented by the vector
 146 $\mathbf{y}_{i,j,t} = [y_{1,i,j,t}, y_{2,i,j,t}]^T$, in which the first coordinate $y_{1,i,j,t}$ was proportional to the natural log of
 147 the ratio of algae to coral, and the second coordinate $y_{2,i,j,t}$ was proportional to the natural log of
 148 the ratio of other to the geometric mean of algae and coral (supporting information, section A1).
 149 The T denotes transpose: throughout, we work with column vectors. Note that both raw and
 150 transformed data are dimensionless.

151 The model

152 The true value $\mathbf{x}_{i,t} = [x_{1,i,t}, x_{2,i,t}]^T$ of the isometric log-ratio transformation of cover of hard corals,
 153 macroalgae and other at site i at time t was modelled by a vector autoregressive process of order 1
 154 (i.e. a process in which the cover in a given year depends only on cover in the previous year), an
 155 approach used in other recent models of coral reef dynamics (Cooper et al., 2015; Gross and
 156 Edmunds, 2015). Unlike previous models, we include a random term representing among-site
 157 variation, and explicit treatment of measurement error (making this a state-space model). The full
 158 model is

$$\begin{aligned}
 \mathbf{x}_{i,t+1} &= \mathbf{a} + \boldsymbol{\alpha}_i + \mathbf{B}\mathbf{x}_{i,t} + \boldsymbol{\varepsilon}_{i,t}, \\
 \boldsymbol{\alpha}_i &\sim \mathcal{N}(\mathbf{0}, \mathbf{Z}), \\
 \boldsymbol{\varepsilon}_{i,t} &\sim \mathcal{N}(\mathbf{0}, \boldsymbol{\Sigma}), \\
 \mathbf{y}_{i,j,t} &\sim t_2(\mathbf{x}_{i,t}, \mathbf{H}, \mathbf{v}),
 \end{aligned}
 \tag{1}$$

159 where all variables and parameters are dimensionless.

160 The column vector \mathbf{a} represents the among-site mean proportional changes in $\mathbf{x}_{i,t}$ evaluated at

161 $\mathbf{x}_{i,t} = \mathbf{0}$. The column vector α_i represents the amount by which these proportional changes for the
162 i th site differ from the among-site mean, and is assumed to be drawn from a multivariate normal
163 distribution with mean vector $\mathbf{0}$ and 2×2 covariance matrix \mathbf{Z} . The 2×2 matrix \mathbf{B} represents the
164 effects of $\mathbf{x}_{i,t}$ on the proportional changes, and can be thought of as summarizing intra- and
165 inter-component interactions such as competition. The column vector $\epsilon_{i,t}$ represents random
166 temporal variation, and is assumed to be drawn from a multivariate normal distribution with mean
167 vector $\mathbf{0}$ and covariance matrix Σ . We assume that there is no temporal or spatial autocorrelation
168 in ϵ , and that ϵ is independent of the among-site variation α .

169 The observed transformed compositions $\mathbf{y}_{i,j,t}$ vary around the corresponding true compositions
170 $\mathbf{x}_{i,t}$ due to both small-scale spatial variation in true composition among transects within a site, and
171 measurement error in estimating composition from a transect. We cannot easily separate these
172 sources of variation because transects were located at different positions in each year, and there
173 were no repeat measurements within transects. Observed log-ratio transformed cover $\mathbf{y}_{i,j,t}$ in the
174 j th transect of site i at time t was assumed to be drawn from a bivariate t distribution (denoted by
175 t_2) with location vector equal to the corresponding $\mathbf{x}_{i,t}$, and unknown scale matrix \mathbf{H} and degrees
176 of freedom ν , so that $\mathbf{y}_{i,j,t}$ has mean vector $\mathbf{x}_{i,t}$ if $\nu > 1$, and covariance matrix $\nu\mathbf{H}/(\nu - 2)$ if
177 $\nu > 2$ (Lange et al., 1989). The bivariate t distribution can be interpreted as a mixture of bivariate
178 normal distributions whose covariance matrices are the same up to a scalar multiple (Lange et al.,
179 1989), and therefore allows a simple form of among-site or temporal variation in the distribution
180 of measurement error or small-scale spatial variation, whose importance increases as the degrees
181 of freedom decrease. Preliminary analyses suggested that it was important to allow this variation,
182 because the model in Equation 1 fitted the data much better than a model with a bivariate normal
183 distribution for $\mathbf{y}_{i,j,t}$ (supporting information, section A3).

184 We make the important simplifying assumptions that \mathbf{B} is the same for all sites, and that the
185 causes of among-site and temporal variation are not of interest. A separate \mathbf{B} for each site, or even
186 a hierarchical model for \mathbf{B} , would be difficult to estimate from the amount of data we have. It
187 might be possible to explain some of the random temporal variation using temporally-varying

188 environmental covariates such as sea surface temperature, and some of the among-site variation
189 using temporally constant covariates such as management strategies (Cooper et al., 2015).
190 However, it is not necessary to do so in order to answer the questions listed at the end of the
191 introduction, and keeping the model as simple as possible is important because parameter
192 estimation is quite difficult. Furthermore, some of the relevant environmental variables may be
193 associated with management strategies, making it difficult to separate the effects of environmental
194 variation and management. For example, although some water quality variables were not strongly
195 associated with protection status (Carreiro-Silva and McClanahan, 2012), unfished reefs were
196 designated as protected areas due to their relatively good condition and are generally found in
197 deeper lagoons with lower and more stable water temperatures than fished reefs (T. R.
198 McClanahan, personal observation).

199 To understand the features of dynamics common to all sites, we plotted the back-transformations
200 from ilr coordinates to the simplex of the overall intercept parameter \mathbf{a} and the columns \mathbf{a}_1 and \mathbf{a}_2
201 of a matrix \mathbf{A} , which is related to \mathbf{B} and describes the effects of current reef composition on the
202 change in reef composition from year to year (Cooper et al., 2015). We plotted \mathbf{A} rather than \mathbf{B}
203 because it leads to a simpler visualization of effects (supporting information, section A4). For
204 example, a point lying to the left of the line representing equal proportions of coral and algae (the
205 1:1 coral-algae isoproportion line) corresponds to a parameter tending to increase coral relative to
206 algae.

207 **Parameter estimation**

208 We estimated all model parameters and checked model performance using Bayesian methods
209 implemented in the Stan programming language (Stan Development Team, 2015), as described in
210 the supporting information (section A5). Stan uses the No-U-Turn Sampler, a version of
211 Hamiltonian Monte Carlo, which can converge much faster than random-walk Metropolis
212 sampling when parameters are correlated (Hoffman and Gelman, 2014). For most results, we
213 report posterior means and 95% highest posterior density (HPD) intervals (Hyndman, 1996),

214 calculated in R (R Core Team, 2015). We showed using simulations that our estimated credible
 215 intervals had close to the specified coverage (section A5.2 and Figure A3).

216 **Long-term behaviour**

217 In the long term (as $t \rightarrow \infty$), the true transformed composition \mathbf{x}^* of a randomly-chosen site will
 218 converge to a stationary distribution, provided that all the eigenvalues of \mathbf{B} lie inside the unit
 219 circle in the complex plane (e.g. Lütkepohl, 1993, p. 10). If the eigenvalues of \mathbf{B} are complex, the
 220 system will oscillate as it approaches the stationary distribution. Details of long-term behaviour
 221 are in the supporting information, section A6.

222 This stationary distribution is the multivariate normal vector

$$\mathbf{x}^* \sim \mathcal{N}(\boldsymbol{\mu}^*, \boldsymbol{\Sigma}^* + \mathbf{Z}^*), \quad (2)$$

223 whose stationary mean $\boldsymbol{\mu}^*$ depends on \mathbf{B} and \mathbf{a} , and whose stationary covariance is the sum of the
 224 stationary within-site covariance $\boldsymbol{\Sigma}^*$ (which depends on \mathbf{B} and $\boldsymbol{\Sigma}$) and the stationary among-site
 225 covariance \mathbf{Z}^* (which depends on \mathbf{B} and \mathbf{Z}).

226 For a fixed site i , the value of α_i is fixed and the stationary distribution is given by

$$\mathbf{x}_i^* \sim \mathcal{N}(\boldsymbol{\mu}_i^*, \boldsymbol{\Sigma}^*), \quad (3)$$

227 whose stationary mean $\boldsymbol{\mu}_i^*$ depends on \mathbf{B} , \mathbf{a} and α_i , and whose stationary covariance matrix is $\boldsymbol{\Sigma}^*$.
 228 Note that \mathbf{B} , which describes intra- and inter-component interactions on an annual time scale,
 229 affects all the parameters of both stationary distributions, and therefore affects both within- and
 230 among-site variability in the long term. Also, the back-transformation of the stationary mean $\boldsymbol{\mu}^*$
 231 of the transformed composition, rather than the arithmetic mean vector of the untransformed
 232 composition, is the appropriate measure of the centre of the stationary distribution (Aitchison,
 233 1989).

234 **How important is among-site variability?**

235 The covariance matrix of the stationary distribution for a randomly-chosen site (Equation 2)
236 contains contributions from both among- and within-site variability. To quantify the contributions
237 from these two sources, we calculated

$$\rho = \left(\frac{|\Sigma^*|}{|\Sigma^* + \mathbf{Z}^*|} \right)^{1/2}, \quad (4)$$

238 (supporting information, section A7), which is the ratio of volumes of two unit ellipsoids of
239 concentration (Kenward, 1979), the numerator corresponding to the stationary distribution in the
240 absence of among-site variation (or for a fixed site, as in Equation 3), and the denominator to the
241 full stationary distribution of transformed reef composition in the region. The volume of each
242 ellipsoid of concentration is a measure of the dispersion of the corresponding distribution. Thus ρ
243 provides an indication of how much of the total variability would remain if all among-site
244 variability was removed. A similar statistic was used by Ives et al. (2003) to measure the
245 contribution of species interactions to stationary variability.

246 **How much variability is there among sites in the probability of low coral** 247 **cover?**

248 For a given coral cover threshold κ , we define $q_{\kappa,i}$ as the long-term probability that site i has coral
249 cover less than or equal to κ . This can be interpreted either as the proportion of time for which the
250 site will have coral cover less than or equal to κ in the long term, or as the probability that the site
251 will have coral cover less than or equal to κ at a random time, in the long term. We set $\kappa = 0.1$,
252 which has been suggested as a threshold for a positive net carbonate budget, based on simulation
253 models and data from Caribbean reefs (Kennedy et al., 2013; Perry et al., 2013; Roff et al., 2015).
254 We calculated $q_{0.1,i}$ for each site numerically (supporting information, section A8). In order to
255 determine whether differences in $q_{0.1,i}$ were related to current coral cover, we plotted $q_{0.1,i}$ against
256 the corresponding sample mean coral cover for each site, over all transects and years. In order to

257 determine whether differences in $q_{0.1,i}$ had obvious explanations, we distinguished between fished
258 and unfished reefs, and patch and fringing reefs. In order to determine whether there was strong
259 spatial pattern in the probability of low coral cover, we calculated spline correlograms (Bjørnstad
260 and Falck, 2001) for a sample from the posterior distribution of $q_{0.1,i}$ (supporting information,
261 section A9).

262 **Which model parameters have the largest effects on the probability of low** 263 **coral cover?**

264 For a given coral cover threshold κ , we define q_κ as the long-term probability that a
265 randomly-chosen site has coral cover less than or equal to κ . This is equal to the expected
266 long-term probability that coral cover is less than or equal to κ over the region, and can be
267 calculated numerically (supporting information, section A8). To find the parameters with the
268 largest effects on q_κ , we calculated its derivatives with respect to each model parameter. As
269 above, we concentrated on $\kappa = 0.1$. However, we also compared results from $\kappa = 0.05$ and
270 $\kappa = 0.20$. The probability q_κ is a function of 12 parameters: all four elements of \mathbf{B} ; both elements
271 of \mathbf{a} ; elements σ_{11} , σ_{21} and σ_{22} of Σ ; and elements ζ_{11} , ζ_{21} and ζ_{22} of \mathbf{Z} . The negative of the
272 gradient vector of derivatives of q_κ with respect to these parameters describes the direction of
273 movement through parameter space in which the probability of low coral cover will be reduced
274 most rapidly, and the elements of this vector with the largest magnitudes correspond to the
275 parameters to which q_κ is most sensitive. To understand why q_κ responds to each model
276 parameter, note that q_κ depends on the parameters $\boldsymbol{\mu}^*$, Σ^* and \mathbf{Z}^* of the stationary distribution
277 (Equation 2), which are in turn affected by the model parameters. We therefore used the chain
278 rule for matrix derivatives (Magnus and Neudecker, 2007, p.108) to break down the derivatives
279 into effects of $\boldsymbol{\mu}^*$, Σ^* and \mathbf{Z}^* on q_κ , and effects of model parameters on $\boldsymbol{\mu}^*$, Σ^* and \mathbf{Z}^*
280 (supporting information, section A10). We also calculated elasticities of q_κ with respect to each
281 parameter, which measure the rate of relative change in q_κ with respect to relative change in the
282 parameter (supporting information, section A11).

283 **How informative is a snapshot about long-term site properties?**

284 In a stochastic system, how much can a “snapshot” survey at a single point in time tell us about
285 the long-term behaviour of the system? For example, are differences among sites that appear to be
286 in good and bad condition likely to be maintained in the long term? To make this question more
287 precise, suppose that we draw a site at random from the region, and at one point in time, draw the
288 true state of the site at random from the stationary distribution for the site. This scenario matches
289 Diamond’s definition of “natural snapshot experiments” as “comparisons of communities
290 assumed to have reached a quasi-steady state” (Diamond, 1986). For simplicity, we assume that
291 we can estimate the true state accurately (for example, by taking a large number of transects). To
292 quantify how informative this is about the long term properties of the site, we computed the
293 correlation coefficients between corresponding components of the true state at a given site at a
294 given time and of stationary mean for that site (supporting information, section A12). If these
295 correlations are high, then a snapshot will be informative about long term properties.

296 **Results**

297 **Overall dynamics**

298 At all sites, the back-transformed posterior mean true states from the model (e.g. Figure 1, grey
299 lines) closely tracked the centres of the distributions of cover estimates from individual transects,
300 although there was substantial among-transect variability at a given site in a given year (e.g.
301 Figure 1, circles). Figure 1 shows two examples, and time series for all sites are plotted in the
302 supporting information, Figures A6 to A35. There were also substantial differences in patterns of
303 temporal change among sites. For example, Kanamai1 (Figure 1a-c), a fished site, had
304 consistently low algal cover and no dramatic changes in cover of any component. In contrast,
305 Mombasa1 (Figure 1d-f), an unfished site, had a sudden decrease in coral cover in 1998, and algal
306 cover was high from 2007 onwards. As a result, Mombasa1 was unusual in that the current

307 estimate of true algal cover was well above the stationary mean estimate (Figure 1e: black circle
308 at end of time series). For most other sites, current estimated true cover was close to the stationary
309 mean (supporting information, Figures A6 to A35, black circles at ends of time series). The
310 uncertainty in true states (Figure 1, grey polygons represent 95% highest posterior density (HPD)
311 credible intervals) was higher during intervals with missing observations (e.g. 2008 in Figure 1).
312 In general, uncertainty in true states (grey polygons) and stationary means (black bars at end of
313 time series) was highest for sites with few observations (e.g. Bongoyo1, Figure A6).
314 The overall intercept parameter \mathbf{a} (Figure 2, green), which describes the dynamics of reef
315 composition at the origin (where each component is equally abundant) was consistent with the
316 observed low macroalgal cover in the region (e.g. Figure 1b, e). The back-transformation of \mathbf{a} lay
317 close to the coral-other edge of the ternary plot, and slightly above the 1:1 coral-other
318 isoproportion line. It therefore represented a strong year-to-year decrease in algae, and a slight
319 increase in other relative to coral, at the origin.

320 Current reef composition acts on year-to-year change in composition (through matrix \mathbf{A}) so as to
321 maintain fairly stable reef composition. The first column \mathbf{a}_1 of \mathbf{A} , which represents the effects of
322 the transformed ratio of algae to coral on year-to-year change in composition, lay (when
323 back-transformed) to the left of the 1:1 coral-algae isoproportion line, above the 1:1 other-algae
324 isoproportion line, and below the 1:1 coral-other isoproportion line (Figure 2, orange). Thus,
325 increases in algae relative to coral resulted in decreases in algae relative to coral and other, and
326 increases in coral relative to other, in the following year. The second column \mathbf{a}_2 of \mathbf{A} , which
327 represents the effects of the transformed ratio of other to algae and coral on year-to-year change
328 in composition, lay (when back-transformed) on the 1:1 coral-algae isoproportion line, below the
329 1:1 other-algae isoproportion line, and below the 1:1 coral-other isoproportion line (Figure 2,
330 blue). Thus, increases in other relative to algae and coral resulted in little change in the ratio of
331 coral to algae, but decreases in other relative to both coral and algae. Consistent with the above
332 interpretation of year-to-year dynamics, every set of parameters in the Monte Carlo sample led to
333 a stationary distribution, since both eigenvalues of \mathbf{B} lay inside the unit circle in the complex

334 plane (supporting information, section A13). The magnitudes of these eigenvalues were smaller
335 than those for a similar model for the Great Barrier Reef (Cooper et al., 2015), indicating more
336 rapid approach to the stationary distribution. There was some evidence for complex eigenvalues
337 of **B**, leading to rapidly-decaying oscillations in both components of transformed reef
338 composition on approach to this distribution. This contrasts with the Great Barrier Reef, where
339 there was no evidence for oscillations (Cooper et al., 2015).

340 **How important is among-site variability?**

341 There was substantial among-site variability in the locations of stationary means (Figure 3,
342 dispersion of points). Stationary mean algal cover was always low, but there was a wide range of
343 stationary mean coral cover. Although our primary focus is not on the causes of among-site
344 variability, there was a tendency for most of the reefs with highest stationary mean coral cover to
345 be patch reefs (Figure 3, circles). In the light of these observations, we experimented with a model
346 in which reef type was included as an explanatory variable. Although the estimated effects of reef
347 type were consistent with lower long-term probabilities of coral cover ≤ 0.1 , including reef type
348 did not improve the expected predictive accuracy of the model (F. Chong, unpublished results),
349 probably because only 482 out of 2665 transects were from patch reefs, and all but one patch
350 reefs had only very short time series (supporting information, Table A1). The stationary means
351 did not clearly separate by management (Figure 3, open symbols fished, filled symbols unfished).
352 The long-term temporal variability around the stationary means was also substantial (Figure 3,
353 green lines). The ρ statistic (Equation 4), which quantifies the posterior mean contribution of
354 within-site variability to the total stationary variability in reef composition in the region, was 0.29
355 (95% HPD interval (0.20, 0.39)), or approximately one third. Thus, while within-site temporal
356 variability around the stationary mean was not negligible, among-site variability in the stationary
357 mean was more important in the long term. As noted above, uncertainty in the location of the
358 stationary means (Figure 3, grey dashed lines) was much higher for reefs with few observations
359 than for reefs with many observations. Nevertheless, most parameters of the model are not

reef-specific, and data from reefs with few observations contribute to the estimation of these. For all three components of variability (within-site, among-site, and measurement error/small-scale spatial variability), variation in algal cover was larger than variation in coral or other. This can be seen in the shapes of the back-transformed unit ellipsoids of concentration (Figure 4: within-site, green; among-site, orange; measurement error and small-scale spatial variability, blue) which were all elongated to some extent along the 1:1 coral-other isoproportion line. This was similar to, but less extreme than, the pattern observed in the Great Barrier Reef (Cooper et al., 2015). The among-site ellipsoid almost entirely enclosed the within-site ellipsoid, consistent with the estimate above that within-site variability contributed only around one-third of the total stationary variability in reef composition. The large estimated measurement error/small-scale spatial variability component was consistent with the substantial observed variability in cover among transects at any given site and time (Figure 1, circles and supporting information, Figures A6 to A35, circles). The low estimated degrees of freedom ν for the bivariate t distribution of measurement error/small-scale spatial variability (posterior mean 2.99, 95% HPD interval (2.64, 3.35)) suggested that some aspect of the process leading to variation in measured composition among transects at a given site was varying substantially over space or time, although we cannot determine the mechanism.

How much variability is there among sites in the probability of low coral cover?

There was also substantial among-site variability in the probability of low coral cover. For a randomly-chosen site, the posterior mean probability of coral cover less than or equal to 0.1 ($q_{0.1}$) in the long term was 0.12 (95% credible interval (0.04, 0.21)). The corresponding site-specific probabilities $q_{0.1,i}$ varied from 8×10^{-5} to 0.52 but were low for most sites, with a strong negative relationship between probability of low coral cover and observed mean coral cover (Figure 5). There was no clear distinction between fished and unfished reefs (Figure 5, open symbols fished, filled symbols unfished). However, probability of low coral cover appeared to be systematically

386 lower on patch reefs, which were mainly in Tanzania (Figures 5 and A1, circles: median of
387 posterior means 2×10^{-3} , first quartile 4×10^{-4} , third quartile 0.04) than on fringing reefs
388 (Figures 5 and A1, triangles: median of posterior means 0.08, first quartile 0.04, third quartile
389 0.11). One site (Ras Iwatine) had a much higher probability of low coral cover than all others, and
390 is relatively polluted compared to other sites in this study, due to high levels of nutrient effluent
391 from a large hotel (T.R. McClanahan, personal observation).

392 There was little evidence for strong spatial autocorrelation in the probability of low coral cover,
393 because the 95% envelope for the spline correlogram included zero for all distances other than
394 261 km to 322 km (supporting information, Figure A38). The general lack of strong spatial
395 autocorrelation reflects the substantial variation in probability of coral cover less than or equal to
396 0.1 ($q_{0.1,i}$) among nearby sites, while the possibility of negative spatial autocorrelation at scales of
397 around 300km may reflect the generally low values of $q_{0.1,i}$ for Tanzanian patch reefs, separated
398 from sites in the north of the study area with generally higher $q_{0.1,i}$ by approximately 300km
399 (Figure A1).

400 **Which model parameters have the largest effects on the probability of low** 401 **coral cover?**

402 Both among-site variability and internal dynamics, particularly of other relative to algae and coral
403 (component 2), were important in determining the probability $q_{0.1}$ of coral cover ≤ 0.1 in the
404 region. Figure 6 shows the direction in parameter space along which the probability of low coral
405 cover will reduce most rapidly (the estimated gradient vector of $q_{0.1}$ with respect to all the model
406 parameters). The four parameters to which $q_{0.1}$ was most sensitive were (in descending order:
407 Figure 6) ζ_{21} (among-site covariance between transformed components 1 and 2), b_{22} (effect of
408 component 2 on next year's component 2), ζ_{22} (among-site variance of component 2), and b_{12}
409 (effect of component 2 on next year's component 1). Although there was substantial variability
410 among Monte Carlo iterations in the values of these derivatives, the rank order of magnitudes was
411 fairly consistent (supporting information, Figure A39). All four most important parameters had

412 positive effects on $q_{0.1}$ (Figure 6), so reducing these parameters will reduce $q_{0.1}$. The effects of
413 within-site temporal variability on the probability of low coral cover were relatively unimportant
414 (Figure 6, derivatives of $q_{0.1}$ with respect to σ_{11} , σ_{21} and σ_{22} all had posterior means close to
415 zero). The signs of the effects of each parameter on $q_{0.1}$, sensitivities for coral cover thresholds
416 0.05 and 0.2, and elasticities, are discussed further in the supporting information (sections A14
417 and A15).

418 **How informative is a snapshot about long-term site properties?**

419 For both components of transformed composition, a snapshot of reef composition at a single time
420 on a randomly-chosen site will be informative about the stationary mean (correlations between
421 true value at a given time and stationary mean: component 1 posterior mean 0.84, 95% HPD
422 interval (0.75, 0.91); component 2 posterior mean 0.82, 95% HPD interval (0.73, 0.90)). This is
423 consistent with the negative relationship between long-term probability of coral cover ≤ 0.1 and
424 observed mean coral cover (Figure 5). Thus, while long-term monitoring of East African coral
425 reefs is important for other reasons, it should be possible to identify those with high conservation
426 value (in terms of benthic composition) from a single survey.

427 **Discussion**

428 In the long term (as $t \rightarrow \infty$), among-site variability dominated within-site temporal variability in
429 East African coral reefs. In consequence, the long-term probability of coral cover ≤ 0.1 varied
430 substantially among sites. This suggests that it is in principle possible to make reliable decisions
431 about the conservation value of individual sites based on a survey of multiple sites at one point in
432 time, and to design conservation strategies at the site level. This was not the only possible
433 outcome: if within-site temporal variability dominated among-site variability, among-site
434 differences would be neither important nor predictable in the long term. Given the large positive
435 effect of among-site variability on the long-term probability of coral cover ≤ 0.1 , reducing

436 among-site variability in compositional dynamics may be an effective conservation strategy.

437 The dominance of among-site variability has important implications for conservation. There was

438 clear evidence for the existence of a stationary distribution of long-term reef composition in East

439 Africa. The overall shape of this distribution (Figure 3) was similar to that estimated by Żychaluk

440 et al. (2012) for a subset of the same data, using a different modelling approach. However, our

441 new analysis shows that this distribution is generated by a combination of spatial and temporal

442 processes, with substantial long-term differences among sites. Thus, the distribution in Żychaluk

443 et al. (2012) may be a good approximation to the long-term distribution for a randomly-chosen

444 site, but there will be much less variability over time in the distribution for any fixed site. In

445 consequence, the sites having the highest long-term conservation value can be identified even

446 from single-survey snapshots, and conservation strategies at the site scale may be possible.

447 Furthermore, in cases where among-site variability in dynamics is dominant, it will be misleading

448 to generalize from observations of a few sites to regional patterns (Bruno et al., 2009).

449 In our study, the sites with the highest long-term conservation value are those with very low

450 long-term probabilities of coral cover ≤ 0.1 (Figure 5), a threshold chosen based on evidence that

451 coral cover ≤ 0.1 is detrimental to reef persistence (Kennedy et al., 2013; Perry et al., 2013; Roff

452 et al., 2015). Many of these sites are Tanzanian patch reefs, which may have maintained high

453 coral cover despite disturbance because of local hydrography (McClanahan et al., 2007), and are

454 priority sites for conservation, with high alpha and beta diversity (Ateweberhan and McClanahan,

455 2016). Thus, it seems likely that sites of high conservation value based on community dynamics

456 may also be sites of high diversity resulting from a combination of physical factors and biological

457 interactions (Huston, 1985; West and Salm, 2003). However, the absence of strong spatial

458 autocorrelation in long-term probabilities of coral cover ≤ 0.1 suggests that it will be necessary to

459 consider conservation value at small spatial scales, rather than simply to identify subregions with

460 high conservation value. Similarly, Vercelloni et al. (2014) found that trajectories of coral cover

461 on the Great Barrier Reef were consistent at the scale of km^2 , but not at larger spatial scales. They

462 argued that it would therefore be appropriate to focus management actions at the km^2 scale. Also,

463 it may be easier to persuade local communities to accept management at such scales than at larger
464 scales (McClanahan et al., 2016).

465 A key result is that if we want to minimize the long-term probability $q_{0.1}$ that a randomly-chosen
466 site has coral cover ≤ 0.1 , we should minimize among-reef variability in dynamics, other things
467 being equal. This is because the centre of the stationary distribution lies outside the set of
468 compositions with coral cover ≤ 0.1 (Supporting Information, Section A14). Conversely, if the
469 centre lay inside this set, then (other things being equal) maximizing among-site variability would
470 minimize $q_{0.1}$. This result is very general, applying to any model of community composition
471 which has a stationary distribution, for which increasing among-site variability increases
472 stationary variability, and for any conservation objective based on a composition threshold. Note
473 that even though our conservation objective is based on coral cover alone, and is therefore
474 one-dimensional, it was strongly affected (through parameters such as ζ_{12} and b_{12}) by processes
475 involving all three components of reef composition. Thus, our multivariate approach provides
476 information that could not be obtained from a one-dimensional model.

477 Conservation strategies that might minimize among-site variability include distributing a fixed
478 amount of human activity such as coastal development or fishing evenly, rather than concentrating
479 it in a few locations. On the other hand, many conservation strategies will affect both the mean
480 dynamics and the among-site variability in dynamics. For example, protecting the sites that are
481 already in the best condition will tend to increase among-site variability, while moving the centre
482 of the stationary distribution away from the set of compositions with coral cover ≤ 0.1 .

483 Minimizing among-site variability in dynamics may conflict with other proposed conservation
484 strategies. For example, it has been suggested that increased beta diversity is associated with
485 lower temporal variability in metacommunities, for at least some taxa, and that regions of high
486 beta diversity may therefore be priority regions for conservation (Mellin et al., 2014). It is likely
487 that increased beta diversity will also be associated with increased among-site variability in
488 dynamics, because different species are likely to have different population-dynamic
489 characteristics. Hence, it may not always be possible to manage for both low among-site

490 variability in dynamics and high beta diversity. It is not yet clear which of these objectives is
491 more important in general. Furthermore, there are many other plausible conservation objectives,
492 such as maximizing the expected number of healthy sites or ensuring that at least one healthy site
493 is present at all times, and different objectives can lead to very different optimal strategies (Game
494 et al., 2008).

495 Our analyses were based on the long-term consequences of current environmental conditions, and
496 may therefore not be relevant if environmental conditions change. For example, if changes in
497 climate or local human activity altered the vector \mathbf{a} so as to transpose the centre of the stationary
498 distribution into the set with coral cover ≤ 0.1 , then maximizing among-site variability would
499 become the best strategy. Since declining coral cover trends have been observed at the regional
500 level (e.g. Côté et al., 2005; De'ath et al., 2012), such a shift in the best strategy may occur. It is
501 therefore better to view a stationary distribution under current conditions as a “speedometer” that
502 tells us about the long-term outcome if these conditions were maintained, rather than as a
503 prediction (Caswell, 2001, p. 30). Furthermore, our model did not include connectivity between
504 sites. Although the absence of evidence for strong spatial autocorrelation in the probability of low
505 coral cover (Supporting Information, Section A9 and Figure A38) suggests that connectivity is
506 relatively unimportant for our analysis, it is possible that either current patterns of connectivity or
507 future changes in these patterns may affect both the interpretation of stationary distributions and
508 the optimal management strategy.

509 In conclusion, our analysis extends the broadly-applicable vector autoregressive approach to
510 community dynamics (reviewed by Hampton et al., 2013) by quantifying random among-site
511 variability in dynamics. This gives a new perspective on the long-term behaviour of the set of
512 communities in a region, as a set of stationary distributions with random but persistent
513 differences. The extent of these differences relative to temporal variability determines how
514 predictable the behaviour of individual sites will be. Since these differences may be associated
515 with differences in conservation value, probabilistic risk assessment based on this approach can
516 be used to suggest conservation strategies at both site and regional scales. At site scales, our

517 approach can be used to identify potential coral refugia, while at regional scales, it can identify
518 the parameters with most influence on conservation objectives.

519 Literature cited

520 Aitchison, J. (1986). *The statistical analysis of compositional data*. Chapman and Hall, London.

521 Aitchison, J. (1989). Measures of location for compositional data sets. *Mathematical Geology*,
522 21:787–790.

523 Ateweberhan, M. and McClanahan, T. R. (2016). Partitioning scleractinian coral diversity across
524 reef sites and regions in the Western Indian Ocean. *Ecosphere*, 7(5):01243.

525 Baker, A. C., Glynn, P. W., and Riegl, B. (2008). Climate change and coral reef bleaching: an
526 ecological assessment of long-term impacts, recovery trends and future outlook. *Estuarine,
527 Coastal and Shelf Science*, 80:435–471.

528 Bjørnstad, O. N. and Falck, W. (2001). Nonparametric spatial covariance functions: Estimation
529 and testing. *Environmental and Ecological Statistics*, 8:53–70.

530 Brook, B. W., O’Grady, J. J., Chapman, A. P., Burgman, M. A., Akçakaya, H. R., and Frankham,
531 R. (2000). Predictive accuracy of population viability analysis in conservation biology. *Nature*,
532 404:385–387.

533 Bruno, J. F., Sweatman, H., Precht, W. F., Selig, E. R., and Schutte, V. G. W. (2009). Assessing
534 evidence of phase shifts from coral to macroalgal dominance on coral reefs. *Ecology*,
535 90(6):1478–1484.

536 Carreiro-Silva, M. and McClanahan, T. R. (2012). Macrobioerosion of dead branching *Porites*, 4
537 and 6 years after coral mass mortality. *Marine Ecology Progress Series*, 458:103–122.

538 Caswell, H. (2001). *Matrix population models: construction, analysis, and interpretation*.
539 Sinauer, Sunderland, MA, second edition.

- 540 Cinner, J. E. and McClanahan, T. R. (2015). A sea change on the African coast? Preliminary
541 social and ecological outcomes of a governance transformation in Kenyan fisheries. *Global*
542 *Environmental Change*, 30:133–139.
- 543 Connell, J. H., Hughes, T. P., and Wallace, C. C. (1997). A 30-year study of coral abundance,
544 recruitment, and disturbance at several scales in space and time. *Ecological Monographs*,
545 67(4):461–488.
- 546 Cooper, J. K., Spencer, M., and Bruno, J. F. (2015). Stochastic dynamics of a warmer Great
547 Barrier Reef. *Ecology*, 96:1802–1811.
- 548 Côté, I. M., Gill, J. A., Gardner, T. A., and Watkinson, A. R. (2005). Measuring coral reef decline
549 through meta-analyses. *Philosophical Transactions of the Royal Society Series B*, 360:385–395.
- 550 De'ath, G., Fabricius, K. E., Sweatman, H., and Puotinen, M. (2012). The 27-year decline of
551 coral cover on the Great Barrier Reef and its causes. *Proceedings of the National Academy of*
552 *Sciences of the USA*, 109:17995–17999.
- 553 Diamond, J. (1986). Overview: laboratory experiments, field experiments, and natural
554 experiments. In Diamond, J. and Case, T. J., editors, *Community ecology*, pages 3–22. Harper
555 & Row, New York.
- 556 Driver, C. C., Oud, J. H. L., and Voelkle, M. C. (2016). Continuous time structural equation
557 modelling with R package ctsem. *Journal of Statistical Software*, in press.
- 558 Egozcue, J. J., Pawlowsky-Glahn, V., Mateu-Figueras, G., and Barceló-Vidal, C. (2003).
559 Isometric logratio transformations for compositional data analysis. *Mathematical Geology*,
560 35(3):279–300.
- 561 Game, E. T., McDonald-Madden, E., Puotinen, M. L., and Possingham, H. P. (2008). Should we
562 protect the strong or the weak? Risk, resilience, and the selection of marine protected areas.
563 *Conservation Biology*, 22(6):1619–1629.

- 564 Ginzburg, L. R., Slobodkin, L. B., Johnson, K., and Bindman, A. G. (1982). Quasiextinction
565 probabilities as a measure of impact on population growth. *Risk Analysis*, 21:171–181.
- 566 Gorrostieta, C., Ombao, H., Bédard, P., and Sanes, J. N. (2012). Investigating brain connectivity
567 using mixed effects vector autoregressive models. *NeuroImage*, 59:3347–3355.
- 568 Gross, K. and Edmunds, P. J. (2015). Stability of Caribbean coral communities quantified by
569 long-term monitoring and autoregression models. *Ecology*, 96:1812–1822.
- 570 Hampton, S. E., Holmes, E. E., Scheef, L. P., Scheuerell, M. D., Katz, S. L., Pendleton, D. E., and
571 Ward, E. J. (2013). Quantifying effects of abiotic and biotic drivers on community dynamics
572 with multivariate autoregressive (MAR) models. *Ecology*, 94(12):2663–2669.
- 573 Hoffman, M. D. and Gelman, A. (2014). The No-U-Turn Sampler: Adaptively setting path
574 lengths in Hamiltonian Monte Carlo. *Journal of Machine Learning Research*, 15:1351–1381.
- 575 Huston, M. (1985). Patterns of species diversity on coral reefs. *Annual Review of Ecology and*
576 *Systematics*, 16:149–177.
- 577 Hyndman, R. J. (1996). Computing and graphing highest density regions. *The American*
578 *Statistician*, 50(2):120–126.
- 579 Ives, A. R., Dennis, B., Cottingham, K. L., and Carpenter, S. R. (2003). Estimating community
580 stability and ecological interactions from time-series data. *Ecological Monographs*,
581 73(2):301–330.
- 582 Kaiser, L. (1983). Unbiased estimation in line-intercept sampling. *Biometrics*, 39(4):965–976.
- 583 Kennedy, E. V., Perry, C. T., Halloran, P. R., Iglesias-Prieto, R., Schönberg, C. H. L., Wissah, M.,
584 Form, A. U., Carricart-Ganivet, J. P., Fine, M., Eakin, C. M., and Mumby, P. J. (2013).
585 Avoiding coral reef functional collapse requires local and global action. *Current Biology*,
586 23:912–918.

- 587 Kenward, M. G. (1979). An intuitive approach to the MANOVA test criteria. *Journal of the Royal*
588 *Statistical Society Series D*, 28(3):193–198.
- 589 Keppel, G., Van Niel, K. P., Wardell-Johnson, G. W., Yates, C. J., Byrne, M., Mucina, L., Schut,
590 A. G. T., Hopper, S. D., and Franklin, S. E. (2012). Refugia: identifying and understanding safe
591 havens for biodiversity under climate change. *Global Ecology and Biogeography*, 21:393–404.
- 592 Lange, K. L., Little, R. J. A., and Taylor, J. M. G. (1989). Robust statistical modeling using the *t*
593 distribution. *Journal of the American Statistical Association*, 84:881–896.
- 594 Lindegren, M., Möllmann, C., Nielsen, A., and Stenseth, N. C. (2009). Preventing the collapse of
595 the Baltic cod stock through an ecosystem-based management approach. *Proceedings of the*
596 *National Academy of Sciences of the USA*, 106(34):14722–14727.
- 597 Lütkepohl, H. (1993). *Introduction to multiple time series analysis*. Springer-Verlag, Berlin, 2nd
598 edition.
- 599 Magnus, J. R. and Neudecker, H. (2007). *Matrix differential calculus with applications in*
600 *statistics and econometrics*. John Wiley & Sons, Chichester, third edition.
- 601 Mateu-Figueras, G., Pawlowsky-Glahn, V., and Egozcue, J. J. (2011). The principle of working
602 on coordinates. In Pawlowsky-Glahn, V. and Buccianti, A., editors, *Compositional data*
603 *analysis: theory and applications*, pages 31–42. John Wiley & Sons, Chichester.
- 604 McClanahan, T. R. and Arthur, R. (2001). The effect of marine reserves and habitat on
605 populations of East African coral reef fishes. *Ecological Applications*, 11(2):559–569.
- 606 McClanahan, T. R., Ateweberhan, M., Muhando, C. A., Maina, J., and Mohammed, M. S. (2007).
607 Effects of climate and seawater temperature variation on coral bleaching and mortality.
608 *Ecological Monographs*, 77(4):503–525.
- 609 McClanahan, T. R., Muthiga, N. A., and Abunge, C. A. (2016). Establishment of community

- 610 managed fisheries' closures in Kenya: early evolution of the tengefu movement. *Coastal*
611 *Management*, 44:1–20.
- 612 McClanahan, T. R., Muthiga, N. A., and Mangi, S. (2001). Coral and algal changes after the 1998
613 coral bleaching: interaction with reef management and herbivores on Kenyan reefs. *Coral*
614 *Reefs*, 19:380–391.
- 615 Mellin, C., Bradshaw, C. J. A., Fordham, D. A., and Caley, M. J. (2014). Strong but opposing
616 β -diversity-stability relationships in coral reef fish communities. *Proceedings of the Royal*
617 *Society of London Series B*, 281:20131993.
- 618 Mumby, P. J., Hastings, A., and Edwards, H. J. (2007). Thresholds and the resilience of
619 Caribbean coral reefs. *Nature*, 450:98–101.
- 620 Mutshinda, C. M., O'Hara, R. B., and Woiwod, I. P. (2009). What drives community dynamics?
621 *Proceedings of the Royal Society of London Series B*, 276:2923–2929.
- 622 Perry, C. T., Murphy, G. N., Graham, N. A. J., Wilson, S. K., Januchowski-Hartley, F. A., and
623 East, H. K. (2015). Remote coral reefs can sustain high growth potential and may match future
624 sea-level trends. *Scientific Reports*, 5:18289.
- 625 Perry, C. T., Murphy, G. N., Kench, P. S., Smithers, S. G., Edinger, E. N., Steneck, R. S., and
626 Mumby, P. J. (2013). Caribbean-wide decline in carbonate production threatens coral reef
627 growth. *Nature Communications*, 4:1402.
- 628 R Core Team (2015). *R: A Language and Environment for Statistical Computing*. R Foundation
629 for Statistical Computing, Vienna, Austria.
- 630 Roff, G., Zhao, J.-X., and Mumby, P. J. (2015). Decadal-scale rates of reef erosion following El
631 Niño-related mass coral mortality. *Global Change Biology*, 21:4415–4424.
- 632 Sandin, S. A., Smith, J. E., DeMartini, E. E., Dinsdale, E. A., Donner, S. D., Friedlander, A. M.,
633 Konotchick, T., Malay, M., Maragos, J. E., Obura, D., Pantos, O., Paulay, G., Richie, M.,

- 634 Rohwer, F., Schroeder, R. E., Walsh, S., Jackson, J. B. C., Knowlton, N., and Sala, E. (2008).
635 Baselines and degradation of coral reefs in the Northern Line Islands. *PLoS ONE*, 3(2):e1548.
- 636 Stan Development Team (2015). Stan: A C++ library for probability and sampling, version 2.7.0.
- 637 Vercelloni, J., Caley, M. J., Kayal, M., Low-Choy, S., and Mengersen, K. (2014). Understanding
638 uncertainties in non-linear population trajectories: a Bayesian semi-parametric hierarchical
639 approach to large-scale surveys of coral cover. *PLoS ONE*, 9(11):e110968.
- 640 West, J. M. and Salm, R. V. (2003). Resistance and resilience to coral bleaching: implications for
641 coral reef conservation and management. *Conservation Biology*, 17(4):956–967.
- 642 Żychaluk, K., Bruno, J. F., Clancy, D., McClanahan, T. R., and Spencer, M. (2012). Data-driven
643 models for regional coral-reef dynamics. *Ecology Letters*, 15:151–158.

644 **Figure legends**

645 Figure 1. Time series of cover of hard corals, macroalgae and other at two of the 30 sites
646 surveyed: Kanamai1 (fished, a-c) and Mombasa1 (unfished, d-f). Circles are observations from
647 individual transects. Grey lines join back-transformed posterior mean true states from Equation 1,
648 and the shaded region is a 95% highest posterior density interval. The back-transformed
649 stationary mean composition for the site is the black dot after the time series and the bar is a 95%
650 highest posterior density interval.

651 Figure 2. Posterior distributions of the back-transformed overall intercept \mathbf{a} (green), effect \mathbf{a}_1 of
652 component 1 (proportional to $\log(\text{algae/coral})$) on year-to-year change (orange), and effect \mathbf{a}_2 of
653 component 2 (proportional to $\log(\text{other/geometric mean}(\text{algae,coral}))$) on year-to-year change
654 (blue).

655 Figure 3. Stationary among- and within-site variation in benthic composition. Grey points:
656 back-transformed stationary means for each site (open circles fished patch, filled circles unfished
657 patch, open triangles fished fringing, filled triangles unfished fringing, posterior means of of
658 stationary means). Grey dashed curves: back-transformed unit ellipsoids of concentration
659 representing uncertainty in stationary means (calculated using sample covariance matrices from
660 Monte Carlo iterations). Green solid curves: back-transformed unit ellipsoids of concentration
661 representing within-site stationary variation (calculated using posterior mean within-site
662 covariance matrix).

663 Figure 4. Back-transformed unit ellipsoids of concentration for stationary within-site covariance
664 Σ^* (green), stationary among-site covariance \mathbf{Z}^* (orange), and measurement error/small-scale
665 spatial variation $\mathbf{vH}/(\mathbf{v} - 2)$ (blue). In each case, 200 ellipsoids drawn from the posterior
666 distribution are plotted, centred on the origin.

667 Figure 5. Long-term probability of coral cover less than or equal to 0.1 at each site against mean
668 observed coral cover across all years. Circles are patch reefs and triangles are fringing reefs.
669 Open symbols are fished reefs and shaded symbols are unfished. Vertical lines are 95% highest
670 posterior density intervals.

671 Figure 6. Elements of the gradient vector of partial derivatives of the long-term probability of
672 coral cover less than or equal to 0.1 with respect to elements of the \mathbf{B} matrix (effects of
673 transformed composition in a given year on transformed composition in the following year), the \mathbf{a}
674 vector (overall intercept, representing among-site mean proportional changes in transformed
675 composition at the origin), the covariance matrix of random temporal variation Σ , and the
676 covariance matrix of among-site variability \mathbf{Z} . For each parameter, the dot is the posterior mean
677 and the bar is a 95% highest posterior density credible interval. For the covariance matrices, the
678 elements σ_{12} and ζ_{12} are not shown, because they are constrained to be equal to σ_{21} and ζ_{21}
679 respectively. The horizontal dashed line is at zero, the no-effect value.

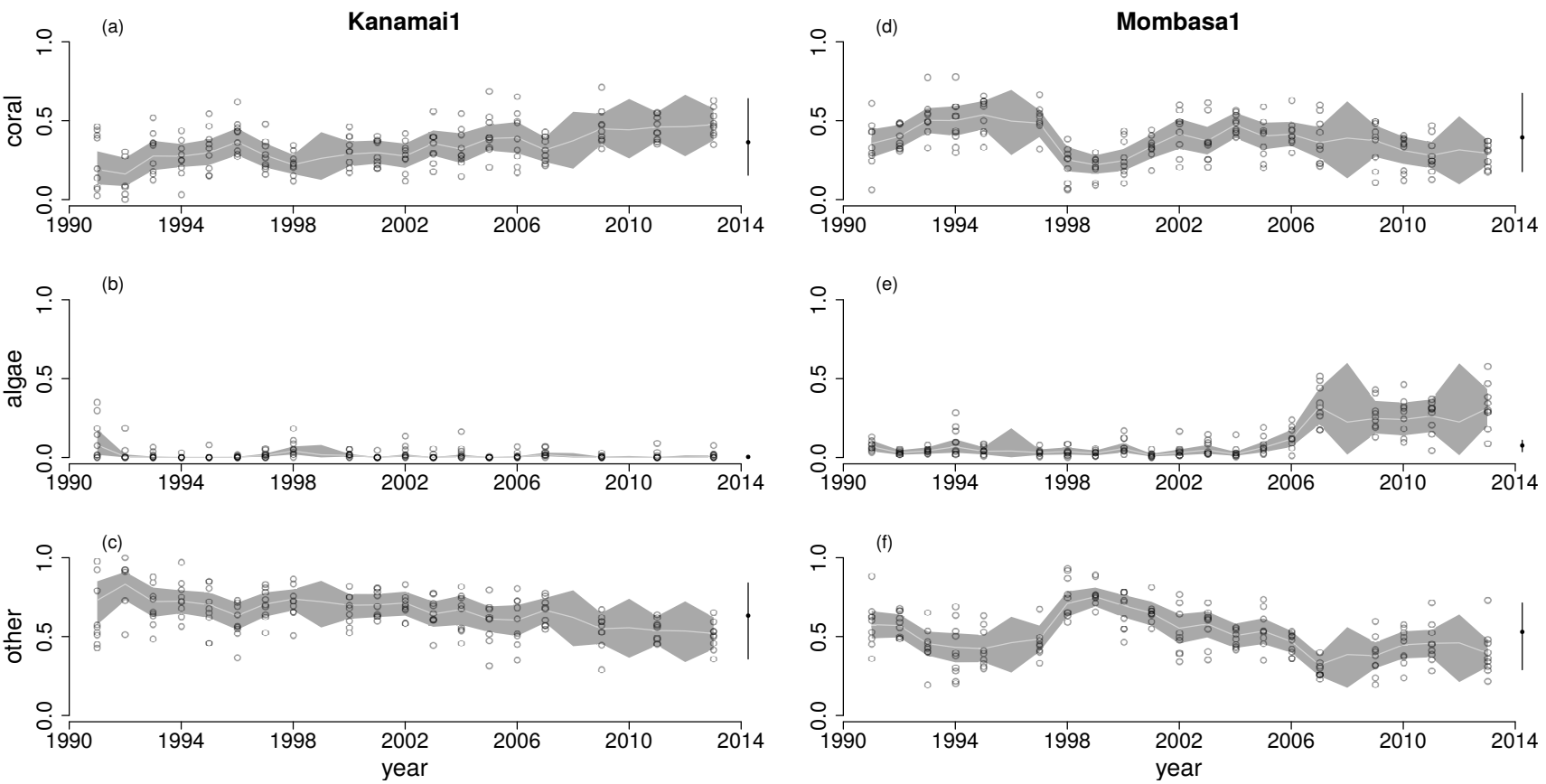


Figure 1:

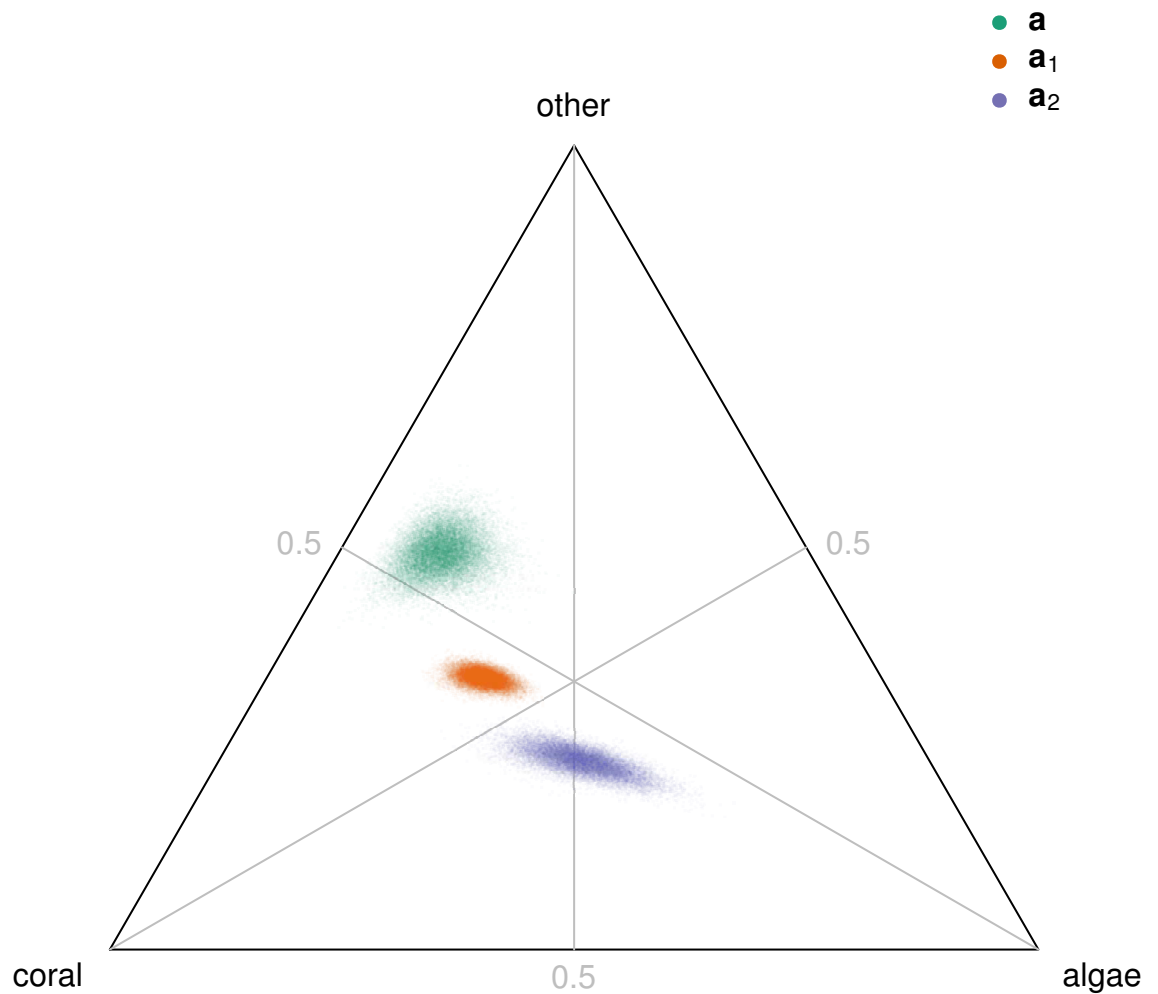


Figure 2:

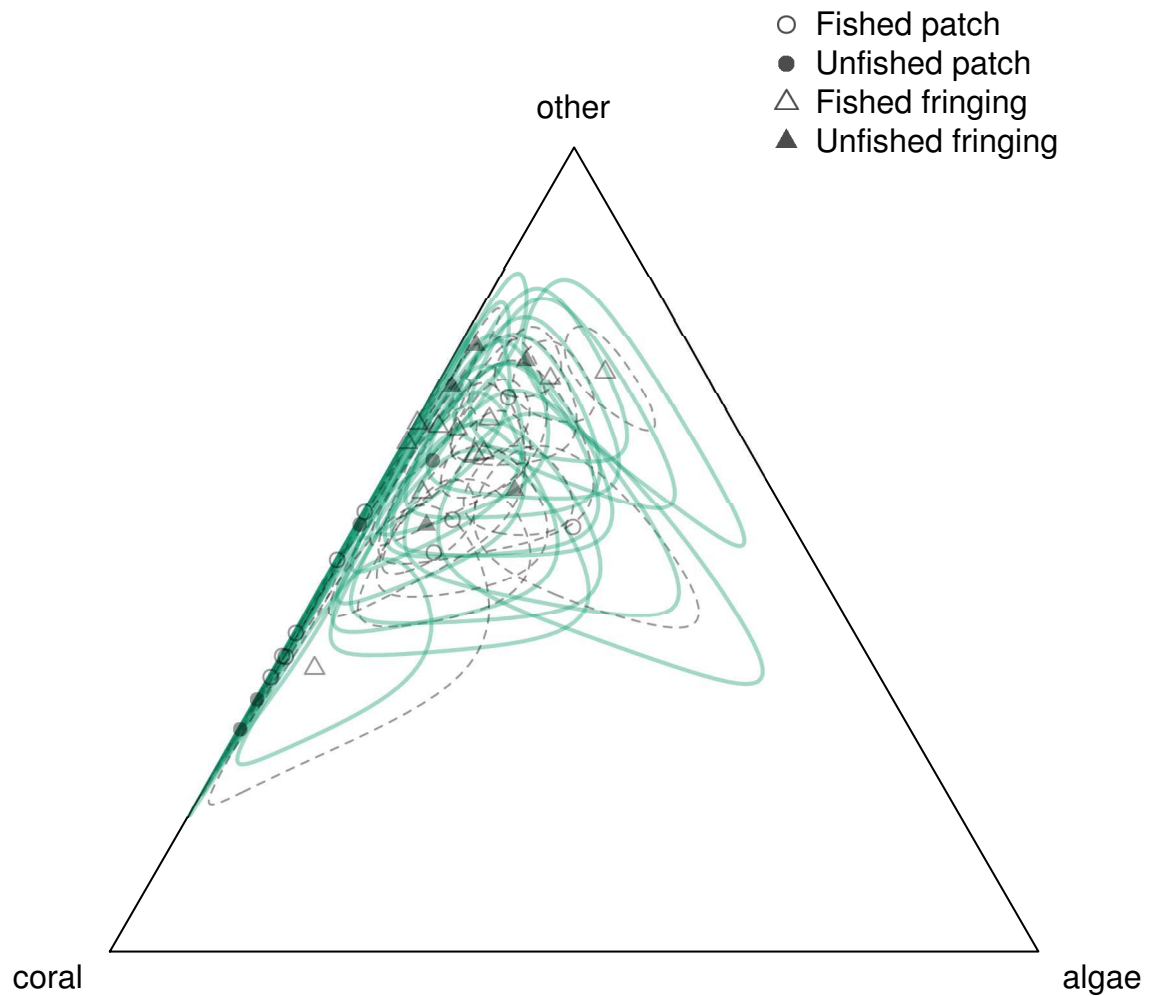


Figure 3:

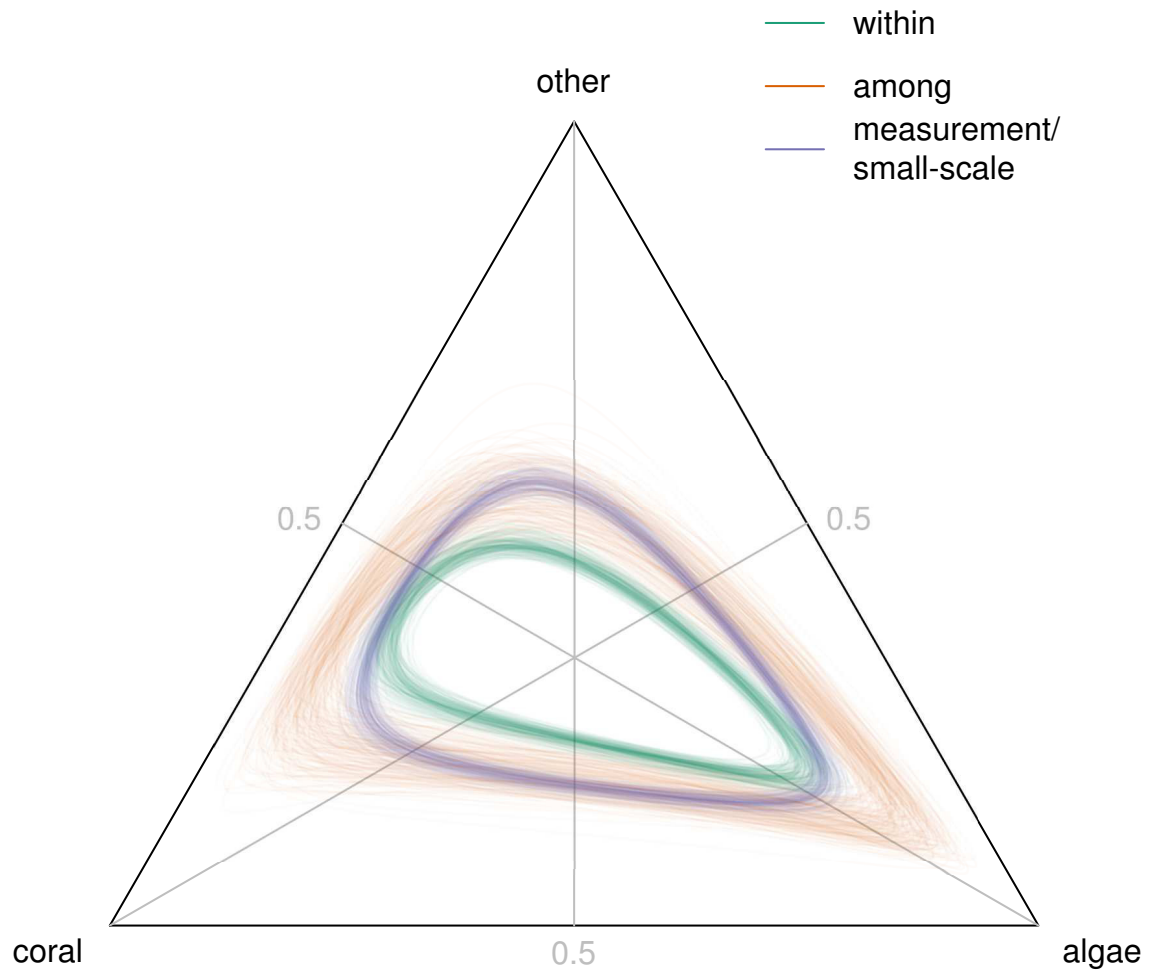


Figure 4:

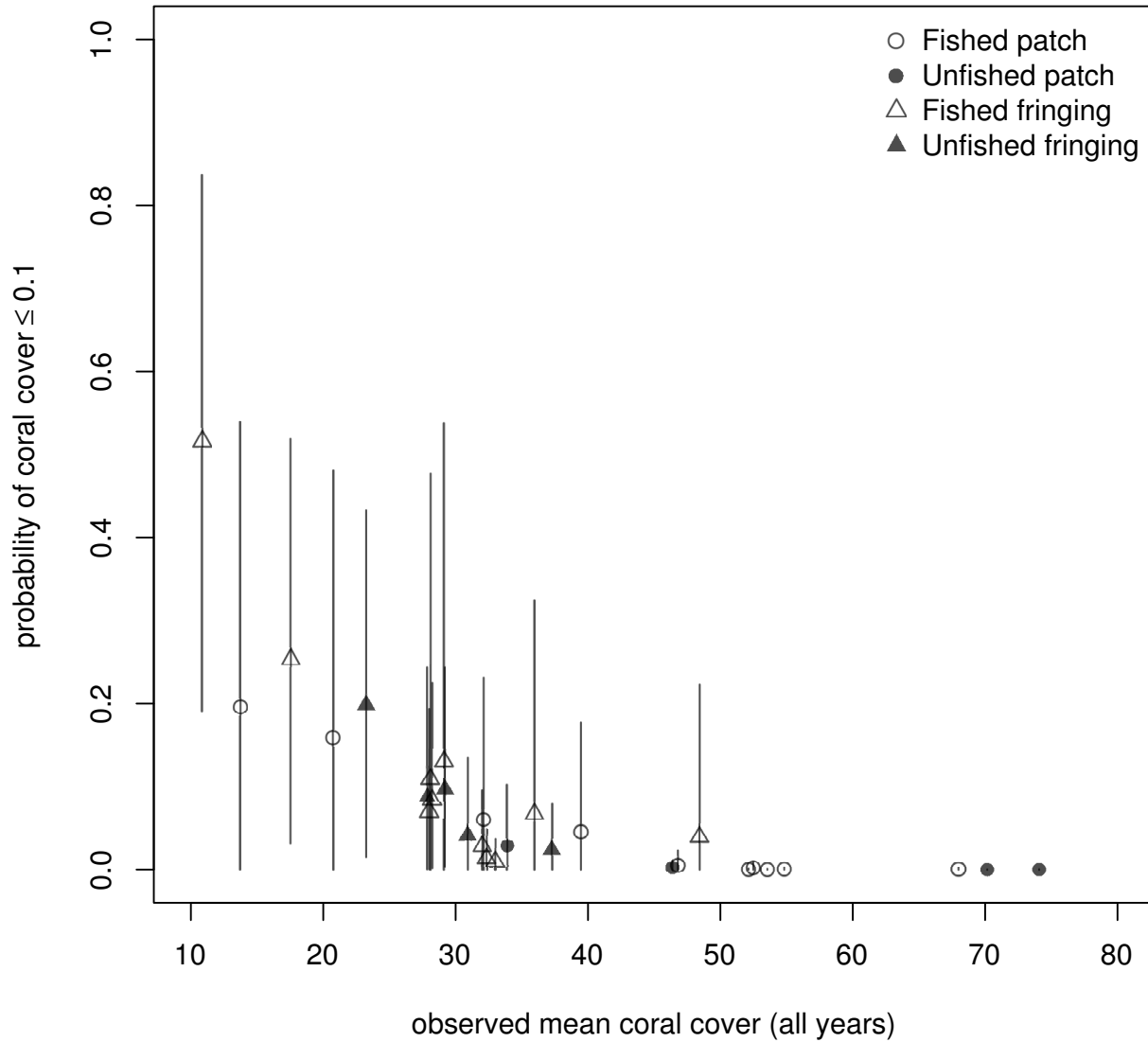


Figure 5:

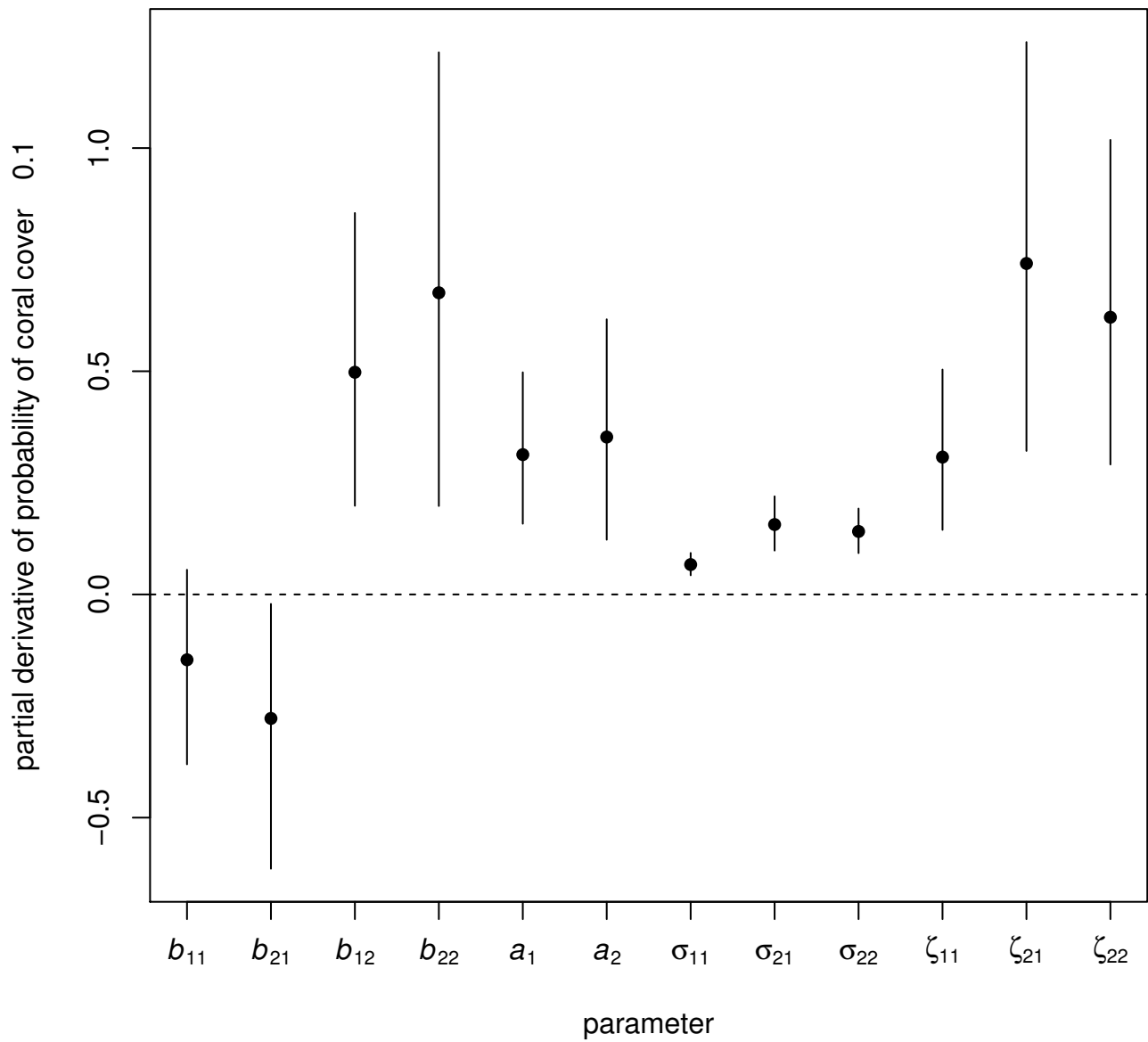


Figure 6: